NONLINEAR HYDRODYNAMIC FORCES ACTING ON CYLINDERS HEAVING ON THE SURFACE OF A FLUID

Tasai, Fukuzo
The Reseach Institute for Applied Mechanics, Kyushu University : Professor

Koterayama, Wataru
The Reseach Institute for Applied Mechanics, Kyushu University : Reseach Associate

https://doi.org/10.5109/6610202

出版情報：Reports of Research Institute for Applied Mechanics. 24 (77), pp.1-39, 1976-11. 九州大学応用力学研究所

Reports of Rerearch Institute for Applied Mechanics
Vol. XXIV, No, 77, 1976

NONLINEAR HYDRODYNAMIC FORCES ACTING ON CYLINDERS HEAVING ON THE SURFACE OF A FLUID*

By Fukuzo TASAI** and Wataru KOTERAYAMA***

Linear and nonlinear hydrodynamic forces are investigated by using two-dimensional cylinders heaving with large amplitude on a free surface. Sections of the cylinders are circle, Lewis form, bulbous bow form (deep and shallow draft) and triangle.

The hydrodynamic forces acting on the cylinders and the concurrent progressive wave heights are measured. First, second and third order forces are obtained from the measured forces by using Fourier analysis. The first order forces and wave heights are compared with values calculated by linear theory. The second-order forces of the circular cylinder are compared with the values calculated by Lee, Parissis and Potash using perturbation method.

Also, the influence of viscous drag force upon the damping coefficient is discussed.

1. Introduction

For the purpose of predicting pitching and heaving motions of a ship in waves, strip method is often used successfully, in which a two-dimensional radiation force and a diffraction force are taken into consideration. The calculated amplitudes of motion together with the phase differences between wave and motion show fairly good agreement with these experimentally obtained. Moreover, though the above method is on the basis of linear theory, the calculated values for the response in regular waves with large steepness give also not so different values from those obtained by model experiments.

When a two-dimensional cylinder performs the heaving oscillation with a large amplitude, it is supposed that the hydrodynamic force acting on the

---

* Condensed and rearranged version of two papers written in Japnese. As to the details of these papers, see the bibliography at the end of this paper.[9),10)]

** Professor, The Reseach Institute for Applied Mechanics, Kyushu University.

*** Reseach Associate, The Reseach Institute for Applied Mechanics, Kyushu University.

cylinder includes the higher order components. Therefore, as for the hydrodynamic force acting on the cylinder heaving with a large amplitude and a circular frequency ω, the following questions may be raised:

1) Can the first order force be estimated with good accuracy by linear theory?

2) Do the second and the third order forces exist? If they do, how large their amplitudes are?

If we can get any knowledge for the first question, it will be useful to know the limit of applicability of linear theory when we intend to modify strip method or develope three dimensional theory for ship motion.

In addition, some knowledges for the second question are useful for the prediction of the nonlinear response of a ship in waves and the wave induced vibration of a ship, especially for the springing.

With regard to the second question, the second order potential theory model was first applied by Kim[1] for the floating triangular cylinder. In general, the second order potential problem can be solved by perturbation method on the assumption that the amplitude of motion is small compared with the beam of a cylinder. Making use of this method, not only the first order force but also the second order force were calculated for the circular cylinder and the U shaped cylinder in pure heaving by Lee[2], for the heaving circular cylinder by Parisis[3], and for the coupled motions of heave and sway, sway and roll, heave and roll by Potash[4].

The main results obtained by their calculations are as follows:

1) Amplitudes of second order forces increase with the increase of the frequency of oscillation.

2) Not only the periodic force but also the time-independent force act on the cylinder. For example, there exists the downward force in the case of heaving.

3) According to the results for the coupled motions by Potash[4], the time-independent horizontal force acts on the cylinder in every case.

Experimental results of the forced oscillation for the two-dimensional cylinder were reported by Tasai[5] (1960). He measured amplitudes of the progressive wave generated by heaving oscillation. Porter[6] (1960) also gave the results on the progressive wave and pressure in heaving. Paulling and Richardson[7] (1962) showed results on the progressive wave, the pressure and the force in heaving, and Vugts[8] (1968) presented those on the progressive wave, the force and the moment in heaving, swaying and rolling motions. But the purposes of their researches were to compare the experimental results with the calculated values by linear theory, the amplitudes of oscillations were small.

In this paper, the progressive wave heights and the hydrodynamic forces acting on the cylinders heaving with large amplitudes were measured. Sections of the cylinders are circle, Lewis form, bulbous bow form (deep and shallow draft) and triangle. The first, the second and the third order forces were obtained from the measured value by using Fourier analysis. The first order forces were compared with the results of calculation by linear theory. In case of circular cylinder the second order forces were compared with the results of calculation given in the papers[2),3),4)]. Furthermore, the influence of viscous drag force upon the damping coefficient was discussed.

2. Model Experiments

Model experiments were performed at a small tank, $L \times B \times D = 60\,m \times 1.5\,m \times 1.5\,m$, of the Research Institute for Applied Mechanics of Kyushu University. Wooden cylinder models were used. In order to realize the two dimensional experiments, length of the models should be taken as close to the width of the tank as possible. The length 1.48 m was finally selected for each model. Their principal dimensions and section-contours are shown in Fig. 1 and the details of the bulbous bow form is shown in Fig. 2.

A forced heaving apparatus is shown in Fig. 3 and Photo. 1.

For the purpose of this research, the motion of model should be simple harmonic motion as precise as possible. Amplitudes of second order and third order motions by this apparatus were obtained from measured motions by using Fourier analysis. They were found to be less than 2 percents and not to be compared with first order motion.

Amplitudes of heaving motions, vertical forces acting on the cylinder and amplitudes of progressive waves were measured. Vertical forces were measured by using two strain-gage type dynamometers (Fig. 3). The amplitudes of progressive waves were measured by making use of two resistance-type wave-probes which were placed in front of the cylinder at a distance of 8 m and apart 0.5 m transversly from each other.

	Circular section		Lewis form section	Bulb section (deep draft)	Bulb section (shallow draft)	Triangular section
Section	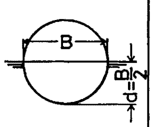		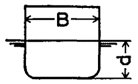	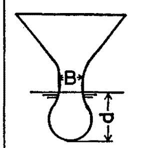	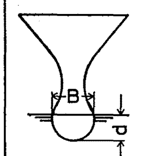	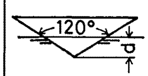
B(m)	0.20	0.12	0.180	0.0626	0.092	0.180
d(m)	0.10	0.06	0.09	0.12	0.066	0.052
$H_0 = B/2d$	1.0		1.0	0.261	0.697	1.732
$\sigma = S/Bd$	0.7854		0.989	1.254	0.950	0.5

Fig. 1 Principal dimensions of cylinders

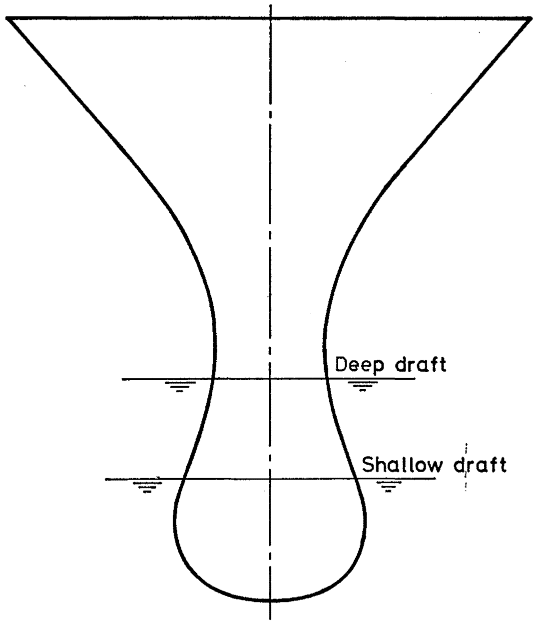

Fig. 2 Details of the bulbous bow section contour

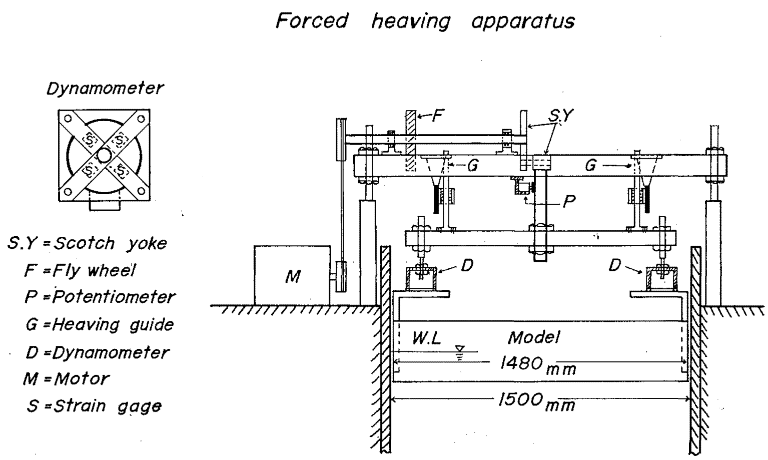

Fig. 3 Forced heaving apparatus

We use following non-dimensional parameter ε which represents the ratio of the heaving amplitude to the half-beam of a cylinder:

$$\varepsilon = Z_a / \frac{B}{2}. \tag{1}$$

The values of the parameter ε and the forced heaving period T in experiments are shown in Table 1 and Table 2.

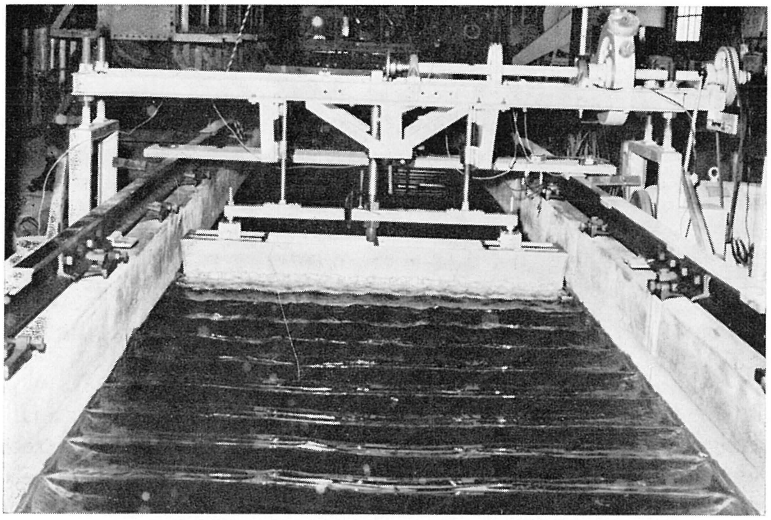

Photo. 1 Forced heaving apparatus

Table 1 ε and forced heaving period T in experiments-Circular cylinder

Model	Z_a (cm)	ε	T (sec)	$\xi_B = \frac{\omega^2}{g} \cdot \frac{B}{2}$
Circular cylinder 1	1.0	0.1	0.5 ~2.0	0.1 ~1.5
(B=0.2m)	2.0	0.2	0.5 ~2.0	0.1 ~1.5
	4.0	0.4	0.5 ~2.0	0.1 ~1.5
	6.0	0.6	0.5 ~2.0	0.1 ~1.5
Circular cylinder 2	2.0	0.333	0.35~1.10	0.2 ~2.0
(B=0.12m)	4.0	0.667	0.37~1.10	0.2 ~1.8
	6.0	1.0	0.37~1.10	0.2 ~1.8
	7.0	1.167	0.37~1.10	0.2 ~1.8

Table 2 ε and forced heaving period T in experiments-Lewis form, Bulbous bow and Triangular cylinder

Model	Z_a(cm)	ε	T(sec)	$\xi_B=\frac{\omega^2}{g}\cdot\frac{B}{2}$
Lewis form cylinder	2.0 4.5 6.0	0.222 0.444 0.667	0.43~1.10	0.3 ~2.0
Bulbous bow cylinder (deep draft)	2.0 4.0 6.0	0.639 1.278 1.917	0.36~1.0	0.2 ~1.0
Bulbous bow cylinder (shallow draft)	2.0 4.0 6.0	0.434 0.870 1.304	0.36~0.96	0.2 ~1.4
Triangular cylinder	2.0 4.0 6.0	0.222 0.444 0.667	0.43~1.10 0.45~1.10 0.45~1.10	0.3 ~2.0 0.3 ~1.8 0.3 ~1.8

3. Analysis of the experimental results and comparison with the theoretical results

Results of experiments are recorded in a data recorder and analized by using a digital computer (FACOM 270-20). Some examples of records of a oscillogram are shown in Fig. 4, Fig. 5 and Fig. 6. The records of forces show that high frequency components (11 Hz-12 Hz) are included in vertical forces, which are caused by the vibration of the forced heaving

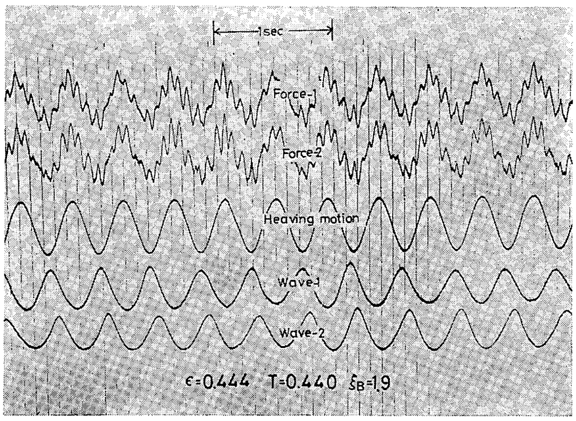

Fig. 4 An illustration of records-Lewis form cylinder

apparatus. Two records of waves in figures are those measured by two wave probes mentioned before. The wave heights were obtained by taking mean values of them.

The method of analysis of the experimental results is shown as follows. The forced heaving motion of the cylinder is given by

$$Z = Z_a \sin \omega t. \tag{2}$$

The force acting on the cylinder can be expressed in a form:

$$F = -M\ddot{Z} + F_w, \tag{3}$$

where M $(=W/g)$ is the mass of the cylinder including attachments of the model and F_w is composed of the buoyancy and the hydrodynamic force.

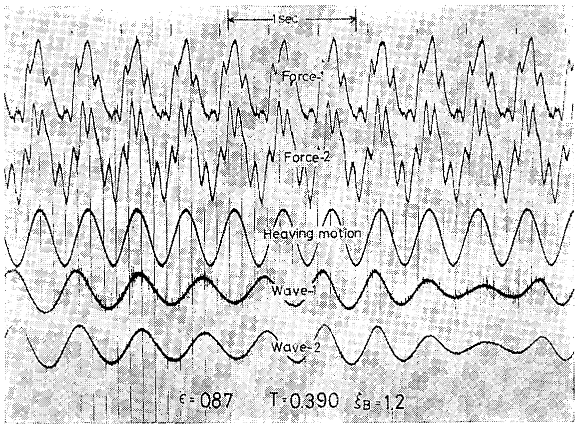

Fig. 5 An illustration of records-Bulbous bow cylinder (shallow draft)

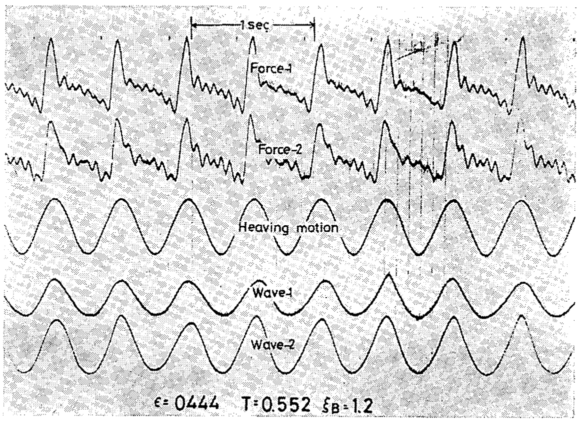

Fig. 6 An illustration of records-Triangular cylinder

Now F_w can be obtained by subtracting $-M\ddot{Z}$ from the measured force F. Moreover, expanding F_W into the Fourier series

$$F_w \sim \sum_{n=0}^{N} F_{wn} = \sum_{n=0}^{N} (A_n \sin n\omega t + B_n \cos n\omega t). \tag{4}$$

we can determine coefficients A_n and B_n as a result.

The restoring force F_B may be written in a polynominal expression and can also be expanded into Fourier series as

$$F_B \sim \rho g \ A_w \sum_{k=0}^{K} f_k \ Z^k = \rho g A_w \ Z_a (C_0 + C_1 \sin \omega t + C_2 \cos 2 \omega t + C_3 \sin 3 \omega t + \cdots\cdots), \tag{5}$$

where A_w is the water plane area when a cylinder is at the rest position. For example, in case of the bulbous bow cylinger (deep draft), F_B is obtained from Fig. 2 as follows,

$$F_B \sim \rho g \ A_w \ Z_a \ [-0.0313\varepsilon + (1+0.0342 \ \varepsilon^2) \sin \omega t + 0.313 \ \varepsilon \cos 2\omega t - 0.0114 \ \varepsilon^2 \sin 3 \ \omega t + \cdots\cdots]. \tag{6}$$

In Table 3, C_0, C_1, C_2 and C_3 for each cylinder are shown.

Combination of equation (1), (4) and (5) leads to the following equation,

$$F_{w1} = Z_a \ [(M_z \ \omega^2 - \rho g \ A_w \ C_1) \sin \omega t - N_z \ \omega \cos \omega t]. \tag{7}$$

Furthermore F_{w1} may be expressed as follows:

$$F_{w1} = |F_{w1}| \sin (\omega t + \delta_{z1}), \tag{8}$$

where δ_{z1} is the phase difference between the heaving motion and the first order force.

Then, using the values of C_1 and F_{w1} which were determined from the analysis of experiments we can obtain values of added mass M_z, damping

Table 3 C_0, C_1, C_2 and C_3

Model	C_0	C_1	C_2	C_3
Circular cylinder	0	$1-0.125\varepsilon^2$	0	$0.042\varepsilon^2$
Bulbous bow cylinder (deep draft)	-0.0313ε	$1+0.0342\varepsilon^2$	0.0313ε	$-0.0114\varepsilon^2$
Bulbous bow cylinder (shallow draft)	-0.038ε	$1-0.044\varepsilon^2$	0.038ε	$0.015\varepsilon^2$
Triangular cylinder (ε=0.222, 0.444)	0.433ε	1.0	-0.433ε	0
Triangular cylinder (ε=0.667)	0.297	1.002	-0.333	-0.0017

coefficient N_z, $|F_{w1}|$ and δ_{z1}.

According to Lee and others[2),3),4)], the first, the second and the third order forces acting on the cylinder are respectively written in forms:

$$\left.\begin{aligned} F_{w1}&=2\rho g\left(\frac{B}{2}\right)^2 L\varepsilon \bar{F}_a{}^{(1)}\sin(\omega t+\delta_{z1}) \\ F_{w2}&=2\rho g\left(\frac{B}{2}\right)^2 L\varepsilon^2 \bar{F}_a{}^{(2)}\sin(2\omega t+\delta_{z2}) \\ F_{w3}&=2\rho g\left(\frac{B}{2}\right)^2 L\varepsilon^3 \bar{F}_a{}^{(3)}\sin(3\omega t+\delta_{z3}) \\ F_{w0}&=2\rho g\left(\frac{B}{2}\right)^2 L\varepsilon^2 \bar{F}_0{}^{(2)}, \end{aligned}\right\} \tag{9}$$

or

$$\left.\begin{aligned} F_{w1}&=\rho gBLZ_a\bar{F}_a{}^{(1)}\sin(\omega t+\delta_{z1}) \\ F_{w2}&=2\rho gLZ_a{}^2\bar{F}_a{}^{(2)}\sin(2\omega t+\delta_{z2}) \\ F_{w3}&=4\rho gL\frac{Z_a{}^3}{B}\bar{F}_a{}^{(3)}\sin(3\omega t+\delta_{z3}) \\ F_0&=2\rho gLZ_a{}^2\bar{F}_0{}^{(2)}, \end{aligned}\right\} \tag{10}$$

The experimental results of $\bar{F}_a{}^{(1)}$, $\bar{M}_z\{=M_z/\rho Bd\sigma L\}$, $\bar{N}_z\{=N_z\sqrt{B/2g}/\rho Bd\sigma L\}$ and δ_{z1} were respectively compared with calculated results by linear theory (Fig. 7∼26).

The results of calculation by linear theory are obtained by using Ursell's

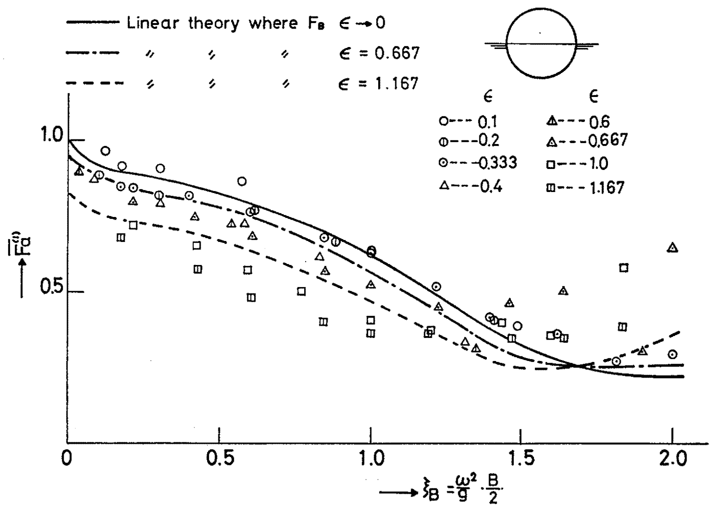

Fig. 7 $\bar{F}_a{}^{(1)}$, First order force–Circular cylinder method[11] in case of the circular cylinder and source distribution method[12] in cases of the other cylinders.

Results obtained from the comparison between theory and experiments are epitomized as follows:

(1) $\bar{F}_a^{(1)}$

The results of calculations and experiments for circular, Lewis form, bulbous bow (deep and shallow draft) and triangular cylinder are presented in Fig. 7~11.

Curves in figures indicate the results of calculations using M_z obtained by linear theory and F_B expressed by equation (5). As seen from the figures, the

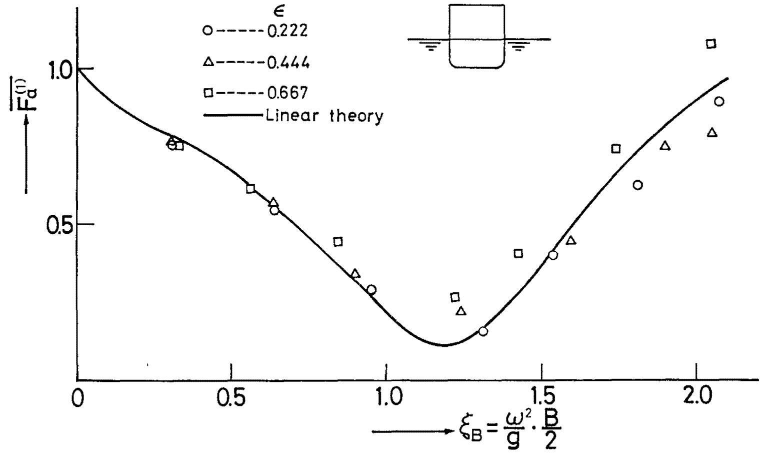

Fig. 8 $\bar{F}_a^{(1)}$, First order force-Lewis form cylinder

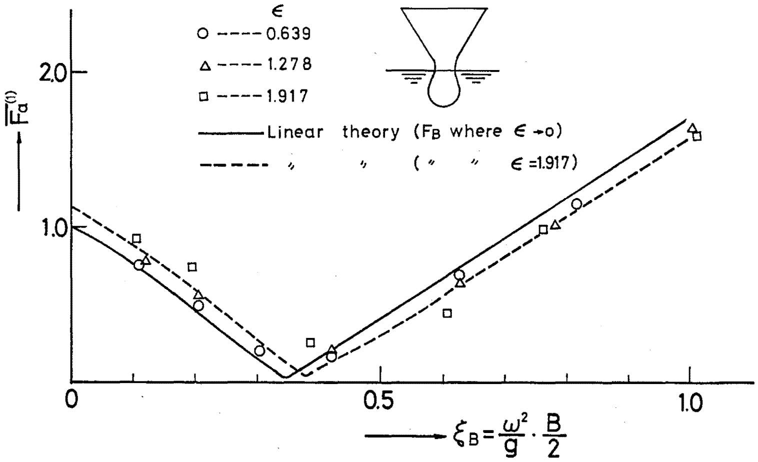

Fig. 9 $\bar{F}_a^{(1)}$, First order force-Bulbous bow cylinder (deep draft) experimental results of $\bar{F}_a^{(1)}$ in case of small ε show good agreement with the calculated results. In case of large ε, the results of experiments on Lewis form and bulbous bow (deep and shallow draft) cylinders show fairly good agreements with the calculated ones using F_B in equation (5), but the results of experiments on circular and triangular cylinder deviate slightly from those of calculated.

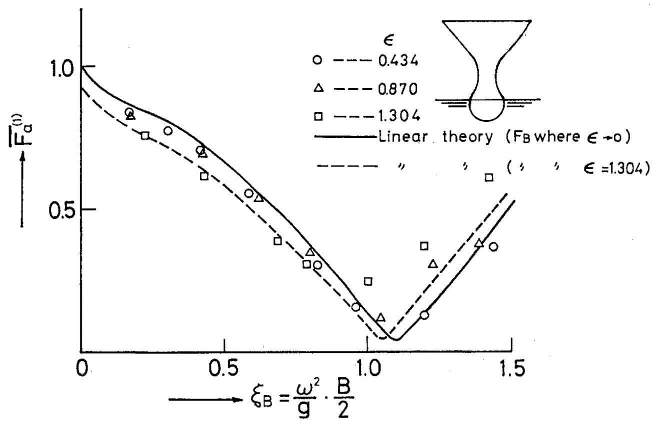

Fig. 10 $\bar{F}_a^{(1)}$, First order force-Bulbous bow cylinder (shallow draft)

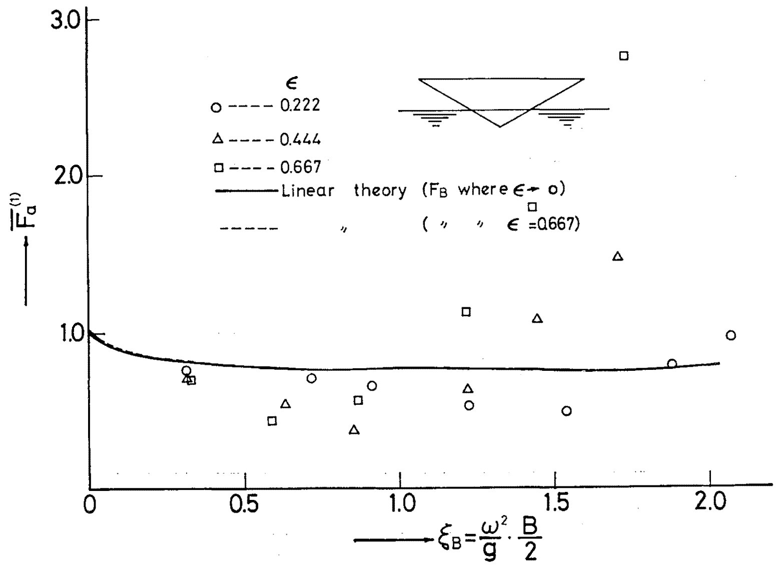

Fig. 11 $\bar{F}_a^{(1)}$, First order force-Triangular cylinder

(2) $\bar{M}_z$

Added mass coefficients $\bar{M}_z$ are presented in Fig. 12~16.

The results of experiments on Lewis form and the bulbous bow cylinder are compared quite well with those of calculation in full range of ε and ξ_B. The results of experiments on circular cylinder show good agreement with calculations in case of $\varepsilon \leqq 0.667$, but the experimental values in case of $\varepsilon \geqq 1.0$ are larger than the calculated ones. When ε is equal to 0.222, in the range of small ξ_B, the experimental values of the triangular section show the same tendency as the calculated one. In the range of large ξ_B, cont-

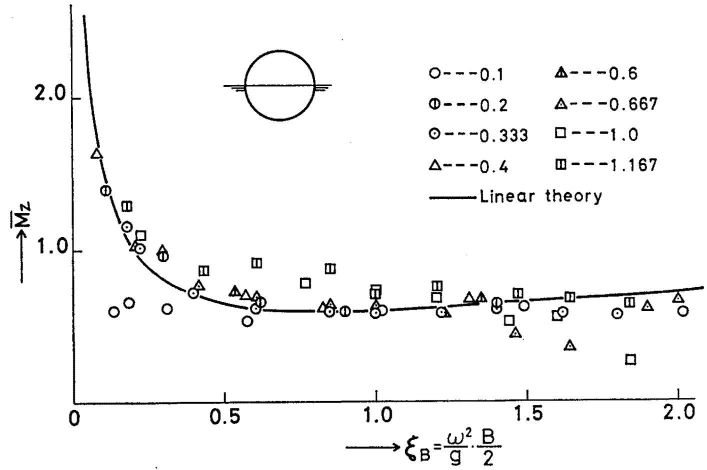

Fig. 12 $\bar{M}_Z$, Added mass coefficient-Circular cylinder

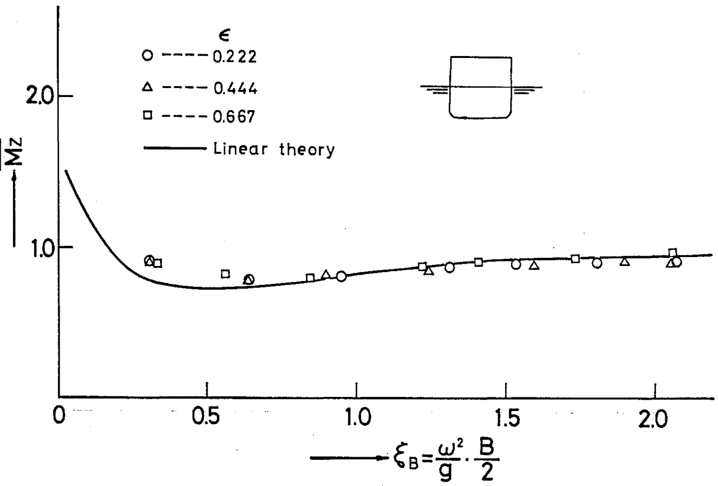

Fig. 13 $\bar{M}_Z$, Added mass coefficient-Lewis form cylinder rary to the prediction of the theory, the experimental values increase with the increase of ξ_B. When ε is equal to 0.444 or 0.667, the larger ε or ξ_B is, the larger the experimental values are. It is ascribed to the fact that the bottom of the model emerges from the water surface.

(3) $\bar{N}_z$

Non-dimensional damping coefficients $\bar{N}_z$ are presented in Fig. 17～21.

As seen from figures, in case of small ε, the experimental values of all models correspond to the calculated ones by linear theory. In case of large ε, experimental values of $\bar{N}_z$ for Lewis form and the bulbous bow (deep and shallow draft) cylinder are larger than the calculated ones. As for the cir-

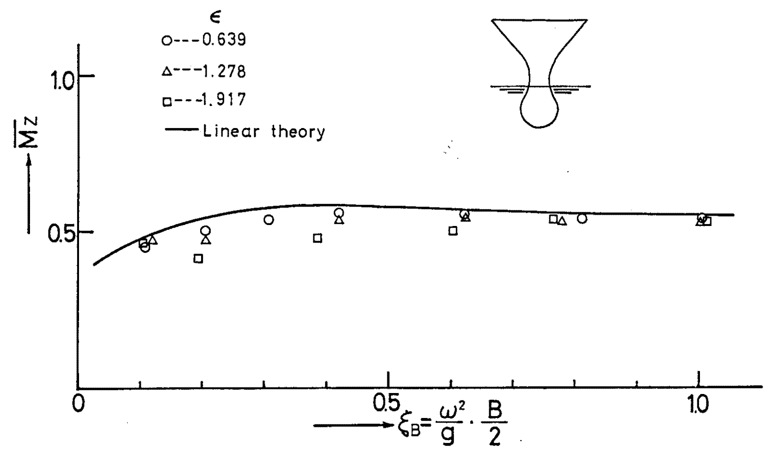

Fig. 14 $\bar{M}_Z$, Added mass coefficient-Bulbous bow cylinder (deep draft)

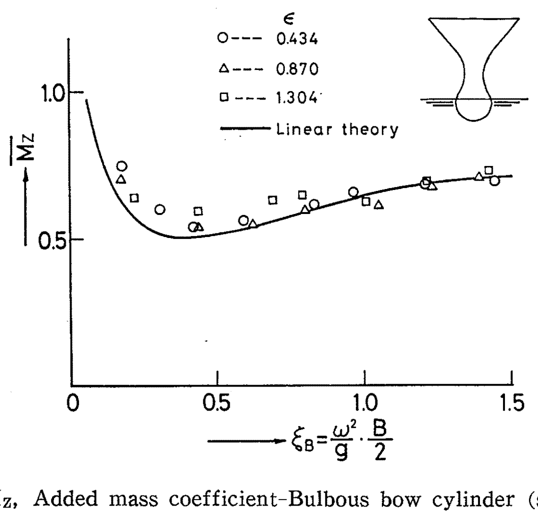

Fig. 15 $\bar{M}_Z$, Added mass coefficient-Bulbous bow cylinder (shallow draft) cular cylinder, the experimental values are smaller than the calculated ones in the range of small ξ_B, and the tendency in the range of large ξ_B is the same as that of Lewis form and the bulbous bow (deep and shallow draft) cylinder. As for the triangular cylinder, the experimental values in case of $\varepsilon < 0.444$ are smaller than the calculated ones, but the experimental values in case of $\varepsilon = 0.667$ abruptly grow larger when ξ_B equals to 1.2, and these facts are possibly caused by the wave breaking phenomena. The calculation by linear theory for the bulbous bow cylinder (deep draft) shows that

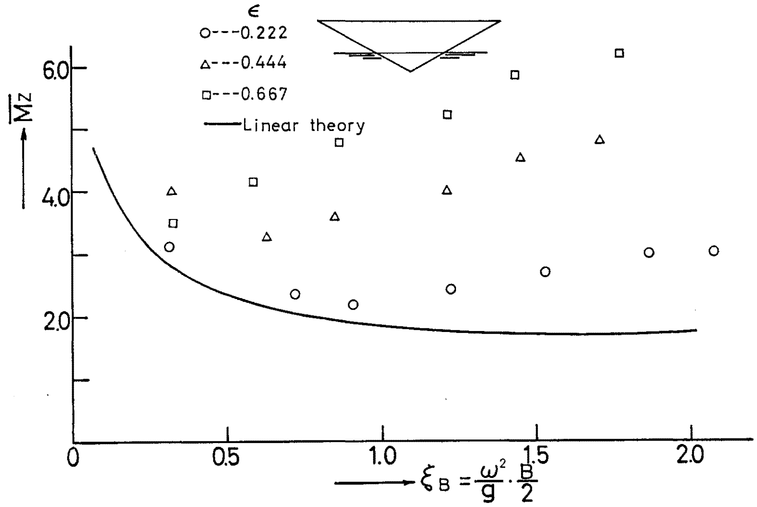

Fig. 16 $\overline{M}_Z$, Added mass coefficient-Triangular cylinder

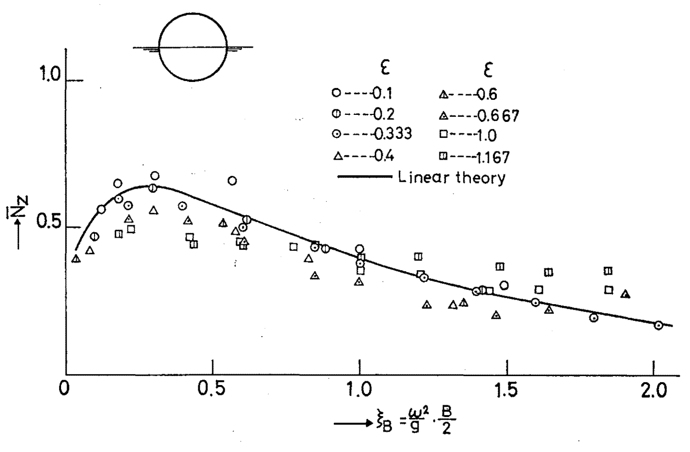

Fig. 17 $\overline{N}_Z$, Non-dimensional damping coefficient-Circular cylinder the waveless frequency exists at $\xi_B=0.22$, but the experimental results do not perfectly agree with the theory because of viscous effects.

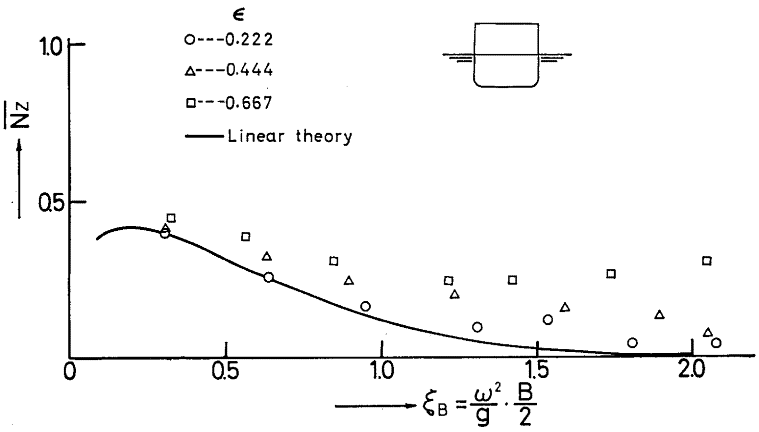

Fig. 18 $\bar{N}_Z$, Non-dimensional damping coefficient-Lewis form cylinder

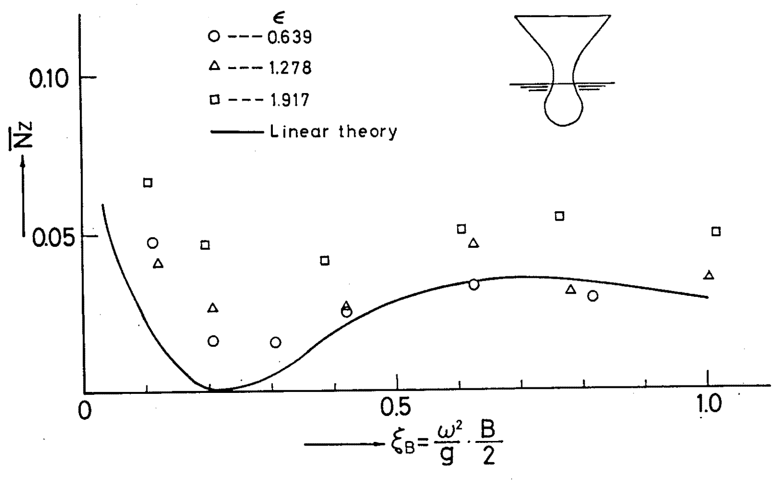

Fig. 19 $\bar{N}_Z$, Non-dimensional damping coefficient-Bulbous bow cylinder (deep draft)

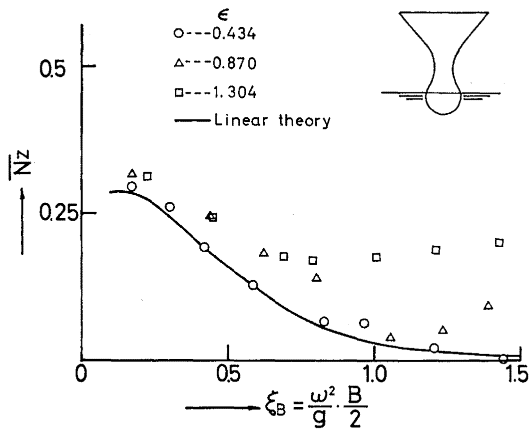

Fig. 20 $\bar{N}_Z$, Non-dimensional damping coefficient-Bulbous bow cylinder (shallow draft)

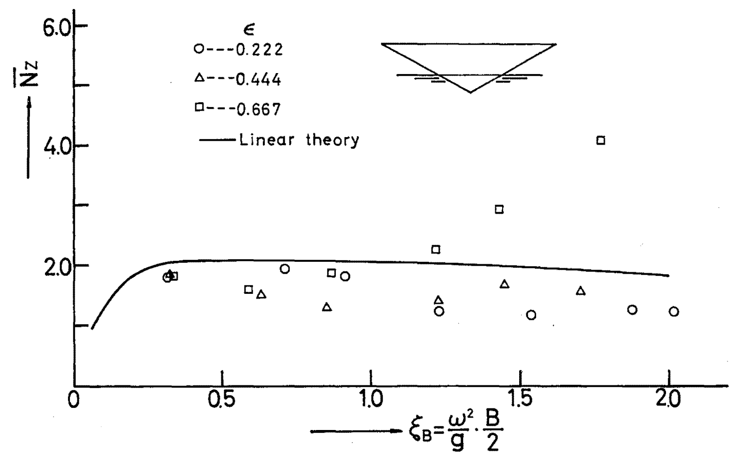

Fig. 21 $\bar{N}_Z$, Non-dimensional damping coefficient-Triangular cylinder

(4) δ_{z1}

Phase differences δ_{z1} between motions and first order forces are presented in Fig. 22~26.

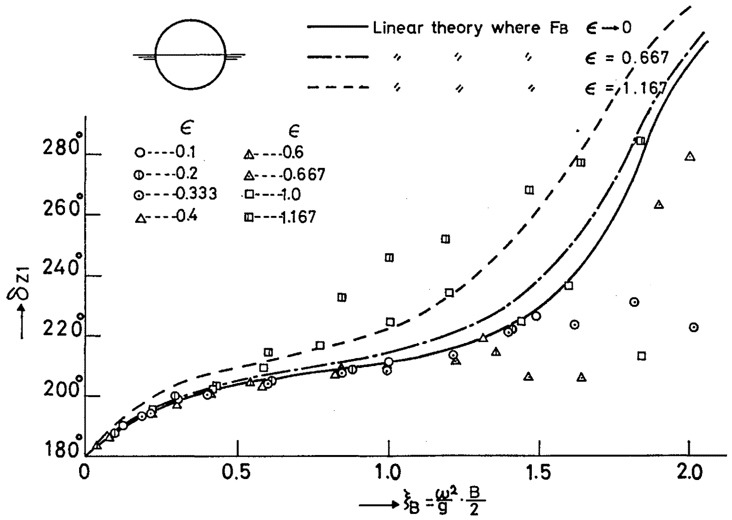

Fig. 22 δ_{Z1}, Phase difference between heaving motion and first order force-Circular cylinder

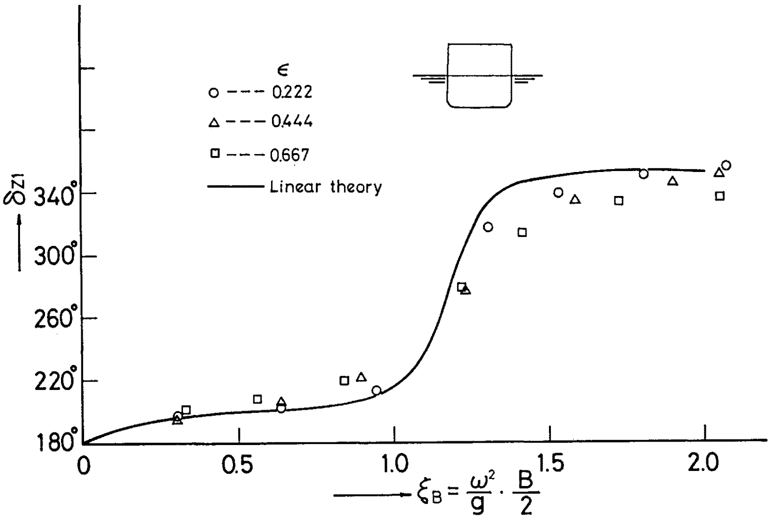

Fig. 23 δ_{Z1}, Phase difference between heaving motion and first order force-Lewis form cylinder

The experimental results show good agreement with linear theory in case of small ε.

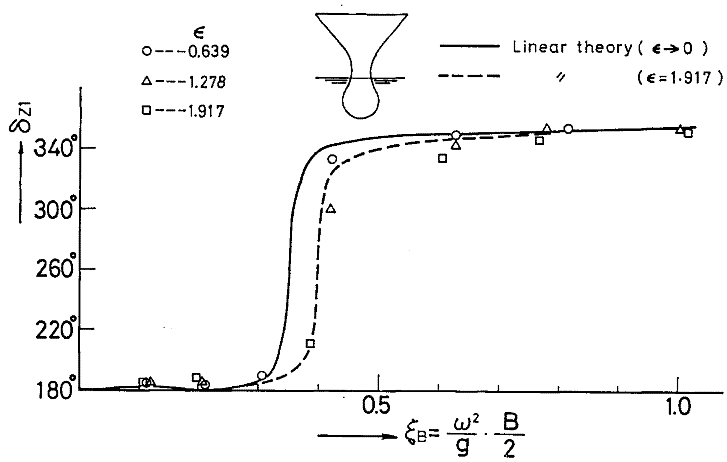

Fig. 24 δ_{Z1}, Phase difference between heaving motion and first order force-Bulbous bow cylinder (deep draft)

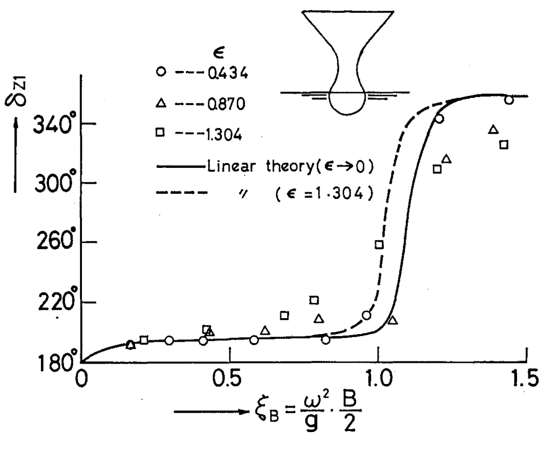

Fig. 25 δ_{Z1}, Phase difference between heaving motion and first order force-Bulbous bow cylinder (shallow draft)

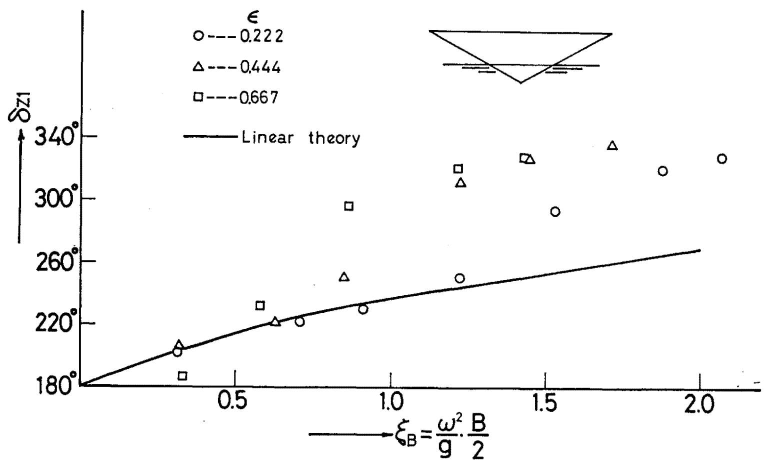

Fig. 26 δ_{Z1}, Phase difference between heaving motion and first order force-Triangular cylinder

(5) $|F_{w2}|/|F_{w1}|$ and $|F_{w3}|/|F_{w1}|$

Experimental values of $|F_{w2}|/|F_{w1}|$ and $|F_{w3}|/|F_{w1}|$ are presented in Fig. 27~36.

As seen from Fig. 8, 9 and 10, each of the first order forces $\bar{F}_a^{(1)}$ of Lewis form and the bulbous bow cylinders has a minimum point at some ξ_B, and therefore, $|F_{w2}|/|F_{w1}|$ and $|F_{w3}|/|F_{w1}|$ of these cylinders each has a maximum point at corresponding ξ_B. As for the circular cylinder, the ex-

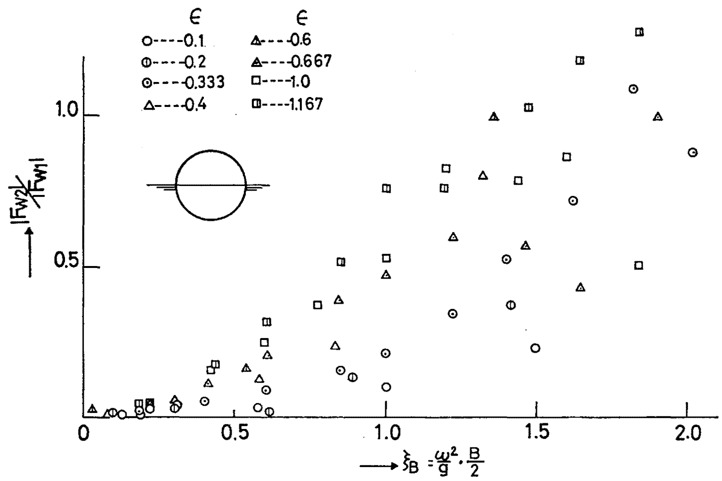

Fig. 27 Ratio of the amplitude of second order force to the one of first order force-Circular cylinder

perimental values increase with the increase of ξ_B. As for the triangular cylinder, the experiments in case of small ε show the same tendency as for the circular cylinder. The experimental values for all models show that $|F_{w2}|/F_{w1}|$ and $|F_{w3}|/|F_{w1}|$ increase with the increase of ε.

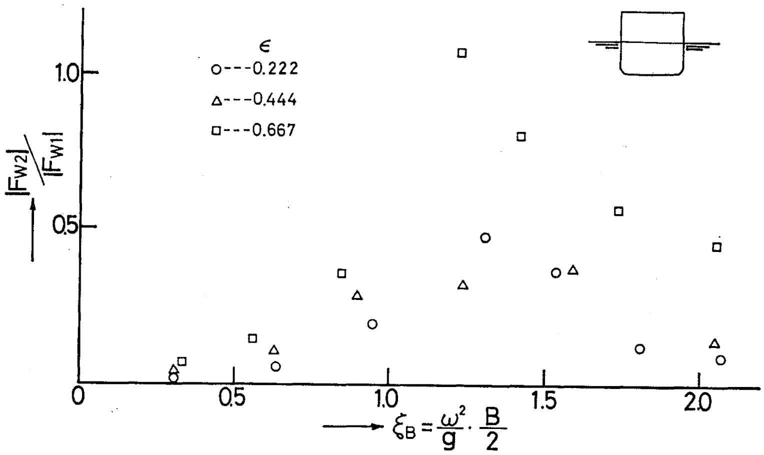

Fig. 28 Ratio of the amplitude of second order force to the one of first order force-Lewis form cylinder

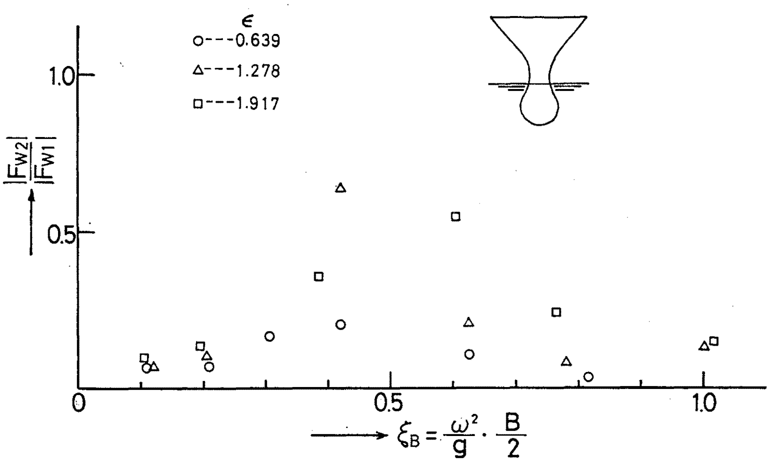

Fig. 29 Ratio of the amplitude of second order force to the one of first order force-Bulbous bow cylinder (deep draft)

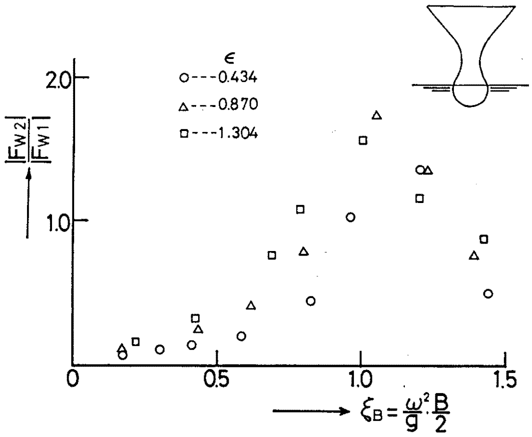

Fig. 30 Ratio of the amplitude of second order force to the one of first order force-Bulbous bow cylinder (shallow draft)

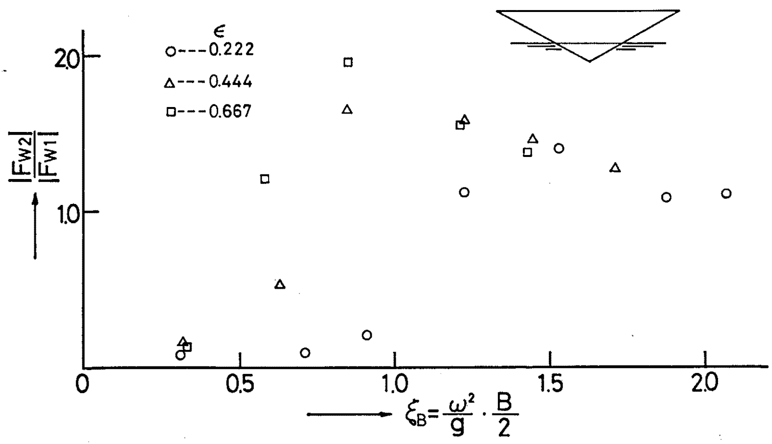

Fig. 31 Ratio of the amplitude of second order force to the one of first order force-Triangular cylinder

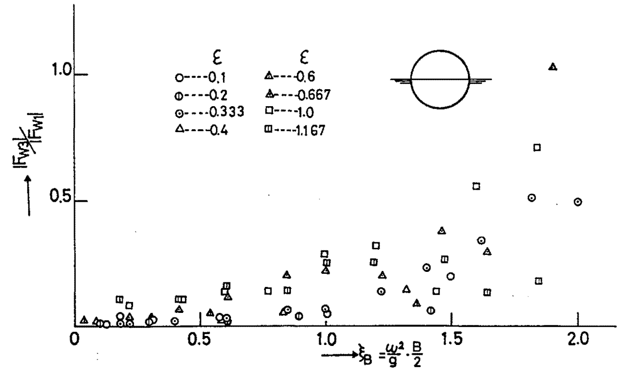

Fig. 32 Ratio of the amplitude of third order force to the one of first order force-Circular cylinder

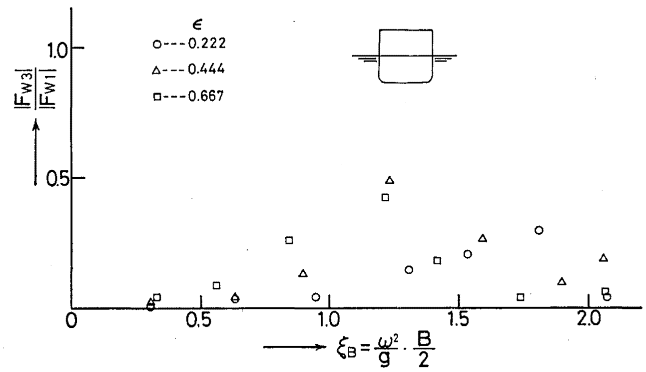

Fig. 33 Ratio of the amplitude of third order force to the one of first order force-Lewis form cylinder

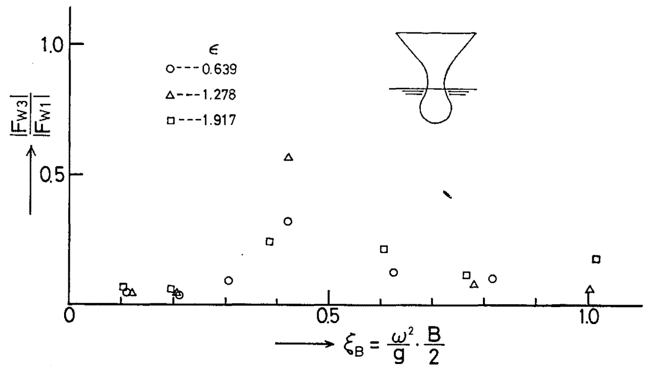

Fig. 34 Ratio of the amplitude of third order force to tne one of first order force-Bulbous bow cylinder (deep draft)

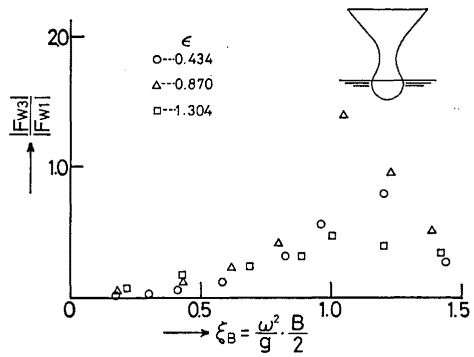

Fig. 35 Raio of the amplitude of third order force to the one of first order force-Bulbous bow cylinder (shallow draft)

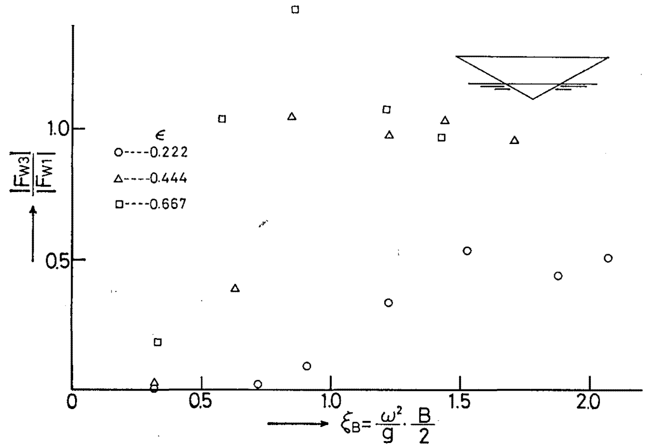

Fig. 36 Ratio of the amplitude of third order force to the one of first order force-Triangular cylinder

(6) $F_a^{(2)}$ and δ_{z2}

Non-dimensional second order forces $\bar{F}_a^{(2)}$ are presented in Fig. 37~41.

The dotted lines in Fig. 39, 40 and 41 indicate the second order forces by the restoring forces. Experiments on Lewis form and the bulbous bow (deep draft) cylinder show that $\bar{F}_a^{(2)}$ are almost independent of ε. As for the circular and the bulbous bow (shallow draft) cylinder, $\bar{F}_a^{(2)}$ increases when ε decreases. On the contrary, for the triangular cylinder $\bar{F}_a^{(2)}$ increases with the increase of ε.

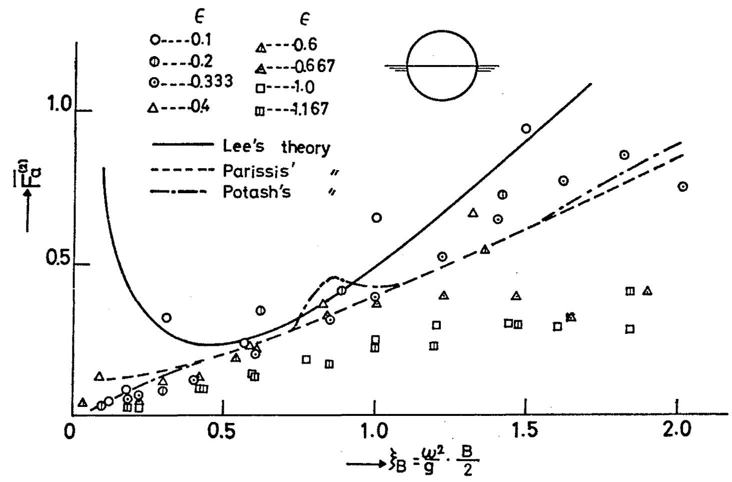

Fig. 37 $\bar{F}_a^{(2)}$, Second order force-Circular cylinder

In Fig. 37, the comparison between the experimental results and calculated ones of the circular cylinder for $\bar{F}_a^{(2)}$ are shown. Three theoretical curves are respectively due to Lee, Parisis and Potash, which were shown in Potash's paper[4]. In case of small ε, the results of experiments show fairly good agreement with the results of calculation. But Lee's calculation in the range of $\xi_B < 0.4$ has a different tendency from the other's calculations and the experimental results for small ε. The experimental results are generally smaller than the theoretical ones and this tendency grows with the increase of ε. The values of $\bar{F}_a^{(2)}$ calculated by the perturbation method give the upper limit of measured values.

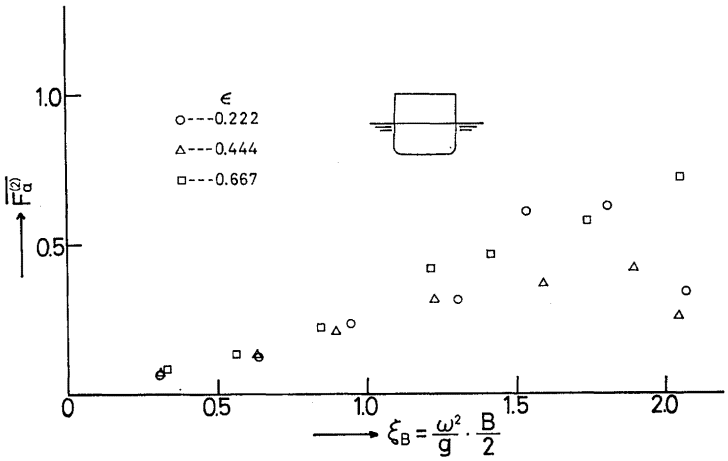

Fig. 38 $\bar{F}_a^{(2)}$, Second order force-Lewis form cylinder

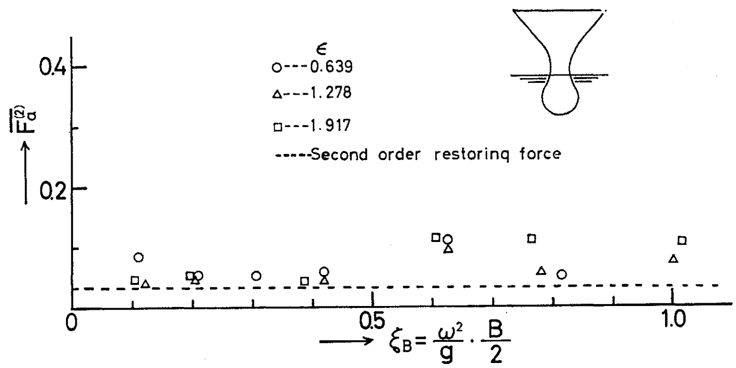

Fig. 39 $\bar{F}_a^{(2)}$, Second order force-Bulbous bow cylinder (deep draft)

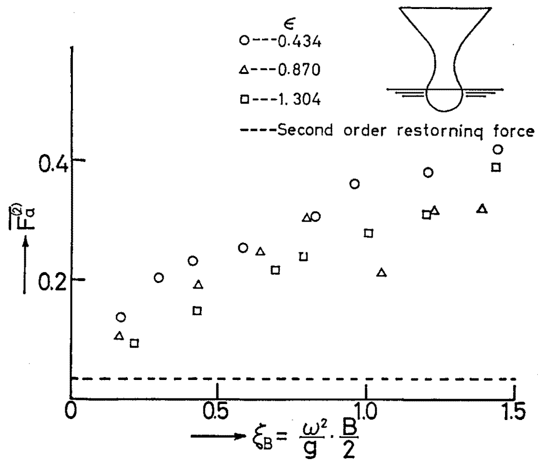

Fig. 40 $\bar{F}_a^{(2)}$, Second order force-Bulbous bow cylinder (shallow draft)

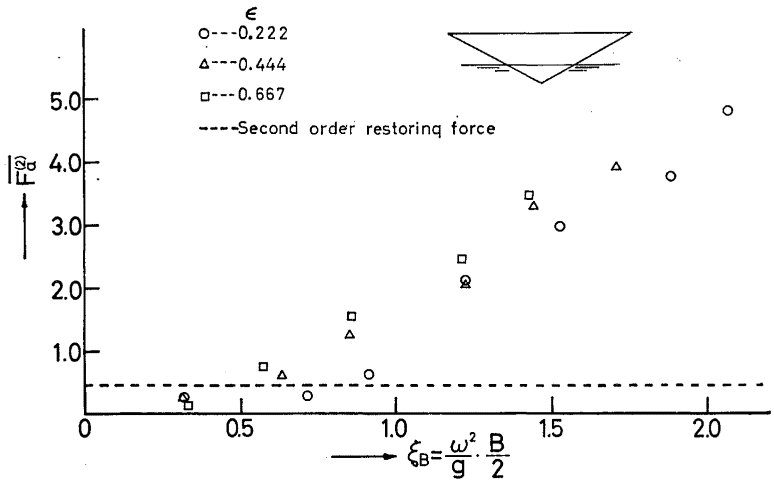

Fig. 41 $\bar{F}_a^{(2)}$, Second order force-Triangular cylinder

Theoretical values of δ_{z2} for the circular cylinder are compared with measured ones in Fig. 42. Theoretical values of δ_{z2} show good agreement with the measured values in range of $\xi_B>0.6$.

(7) F_0

Experimental values of time independent sinking force F_0 are presented in Fig. 43~47.

As for the circular cylinder, the results of experiments are compared with the calculation by perturbation theory. In case of small ε, the experimental values show good agreement with the calculated ones (Fig. 43).

(8) $\bar{A}_1$, $\bar{A}_2$, $\bar{A}_3$,

We put the displacement of progressive waves in a form,

$$h=h_1\cos(\omega t+\delta_{w1})+h_2\cos(2\omega t+\delta_{w2})+ h_3\cos(3\omega t+\delta_{w3})+\cdots\cdots\cdots, \quad (11)$$

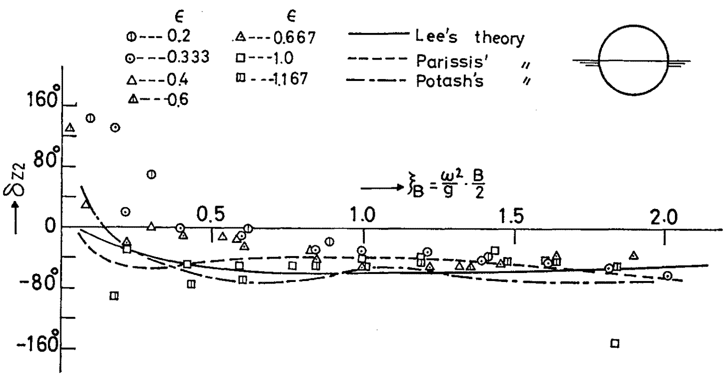

Fig. 42 δ_{Z2}, Phase difference between heaving motion and second order force-Circular cylinder

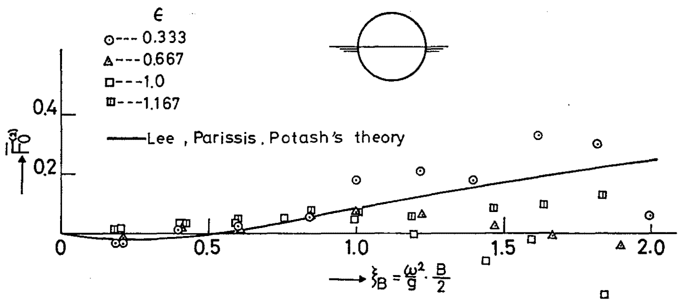

Fig. 43 $\bar{F}_0^{(2)}$, Time-independent sinking force-Circular cylinder

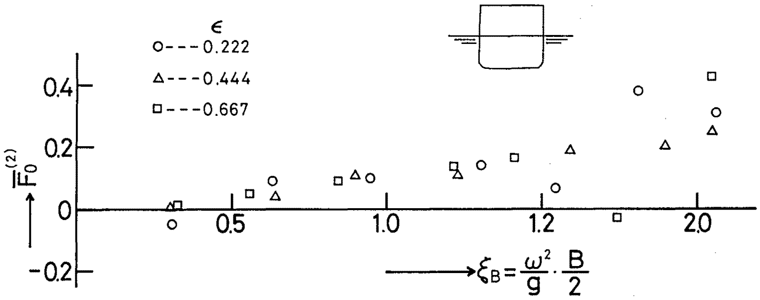

Fig. 44 $\bar{F}_0^{(2)}$, Time-independent sinking force-Lewis form cylinder

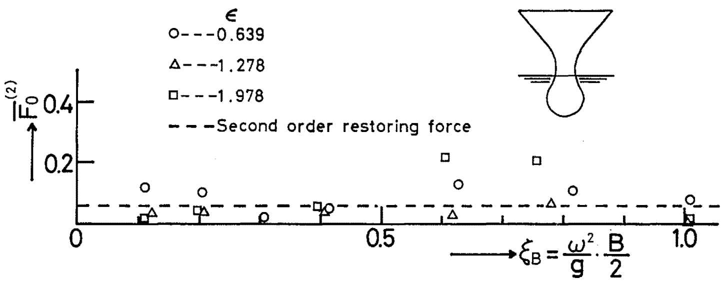

Fig. 45 $\bar{F}_0^{(2)}$, Time-independent sinking force-Bulbous bow cylinder (deep draft)

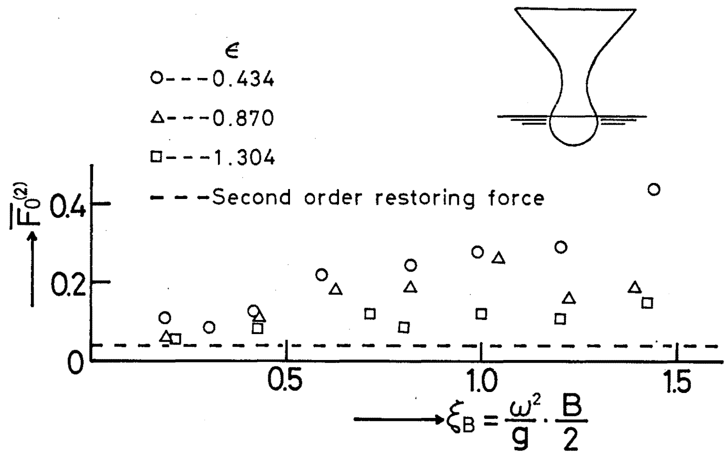

Fig. 46 $\bar{F}_0^{(2)}$, Time-independent sinking force-Bulbous bow cylinder (shallow draft)

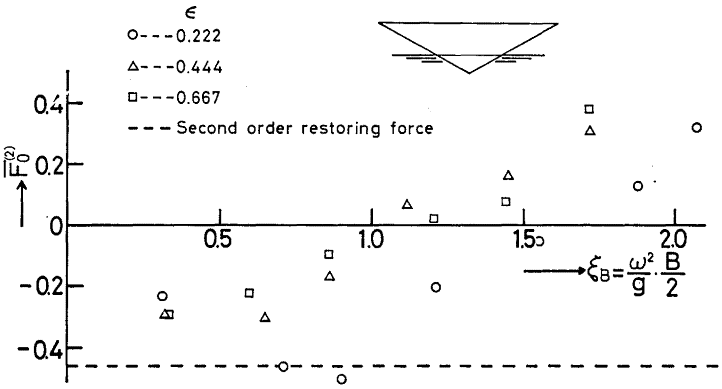

Fig. 47 $\bar{F}_0^{(2)}$, Time-independent sinking force-Triangular cylinder

Then we show $\bar{A}_1=h_1/Z_a$ in Fig. 48~52, and $\bar{A}_2=h_2/Z_a$, $\bar{A}_3=h_3/Z_a$ in Fig. 53~57. The experimental values of $\bar{A}_1$ are compared with the calculated ones by linear theory. The differences between theoretical values and measured ones of $\bar{A}_1$ increase with the increase of ε and ξ_B. The experimental values of $\bar{A}_2$, $\bar{A}_3$ are much smaller than $\bar{A}_1$.

4. Viscous effect on N_z

Values of $\bar{A}_1$, which were calculated by making use of the experimental results N_z given in Fig. 17~21 and the theoretical relation of $N_z=\frac{\rho g^2}{\omega^2}\bar{A}_1^2 L$,

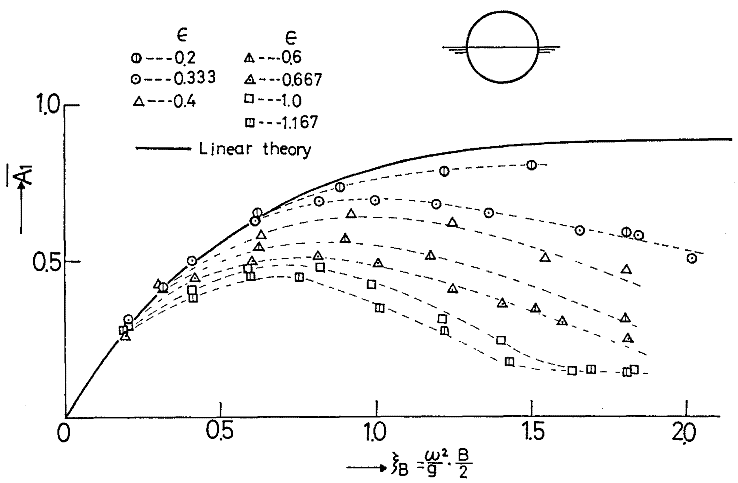

Fig. 48 $\bar{A}$ of first order wave-Circular cylinder were larger than the values of measured $\bar{A}_1$ shown in Fig. 48~52. Especially in case of large ξ_B, the difference is considerably large. From these results, it is inferred that in case of large ξ_B not only the wave-making but also the viscous components and the components due to wave breaking phenomena are included in N_z.

In this paper, the difference between the measured N_z and the calculated N_z by using measured $\bar{A}_1$ is assumed to be caused by the viscous force. It is very difficult to calculate the viscous force exactly. Then introducing the analogy of the oscillating drag force, we assume the viscous force F_v to be expressed as follows:

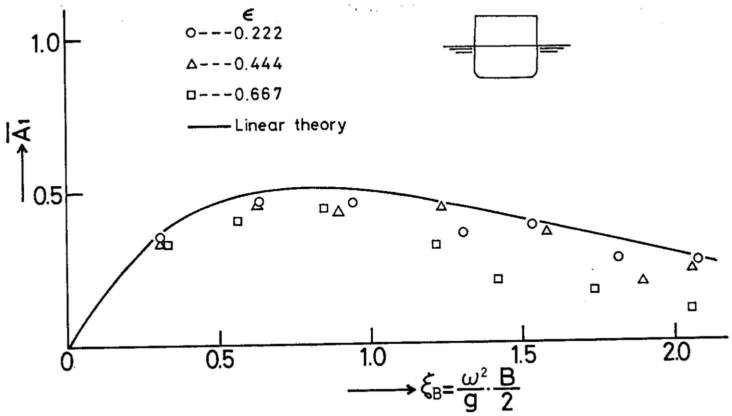

Fig. 49 Ā of first order wave-Lewis form cylinder

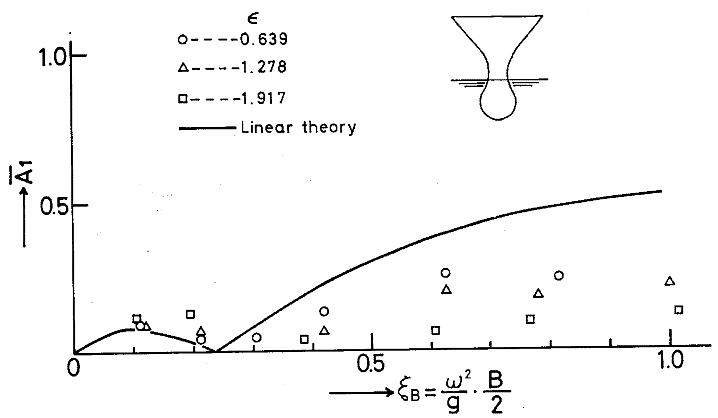

Fig. 50 Ā of first order wave-Bulbous bow cylinder (deep draft)

$$F_v \doteqdot -\frac{1}{2}\rho A_w C_D \dot{Z}|\dot{Z}| \tag{12}$$

Generally, the viscous drag coefficient C_D is thought to be a function of Z_a, ω and t. Substituting equation (2) into equation (12), we obtain the following equation:

$$F_v \doteqdot -\frac{1}{2}\rho A_w C_D \omega^2 Z_a{}^2 \cos\omega|\cos\omega t|. \tag{13}$$

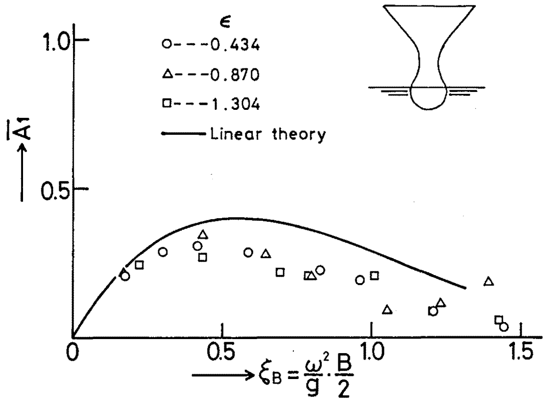

Fig. 51 Ā of first order wave-Bulbous bow cylinder (shallow draft)

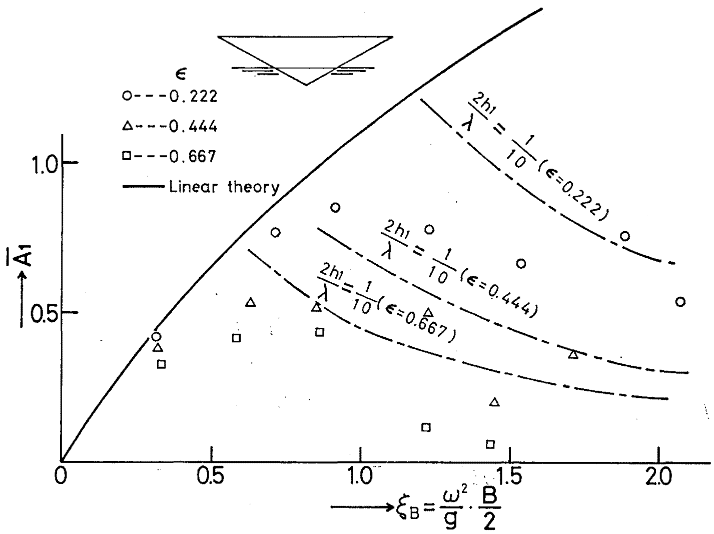

Fig. 52 Ā of first order wave-Triangular cylinder

Expansion of F_v into Fourier series leads to following equation,

$$F_v \sim -\frac{1}{2}\rho A_w C_D \omega^2 Z_a^2 \left(\frac{8}{3\pi}\cos\omega t + \frac{8}{15\pi}\cos 3\omega t + \cdots\cdots\cdots\cdots \right), \quad (14)$$

where C_D is assumed to be independent of t.

Since $\bar{N}_z$ is related to the first order force with the frequency ω, the first term of equation (14) should be adopted, and we can put approximately

$$F_{v1} \doteqdot -\frac{1}{2}\rho A_w C_D \omega^2 Z_a^2 \frac{8}{3\pi}\cos\omega t. \quad (15)$$

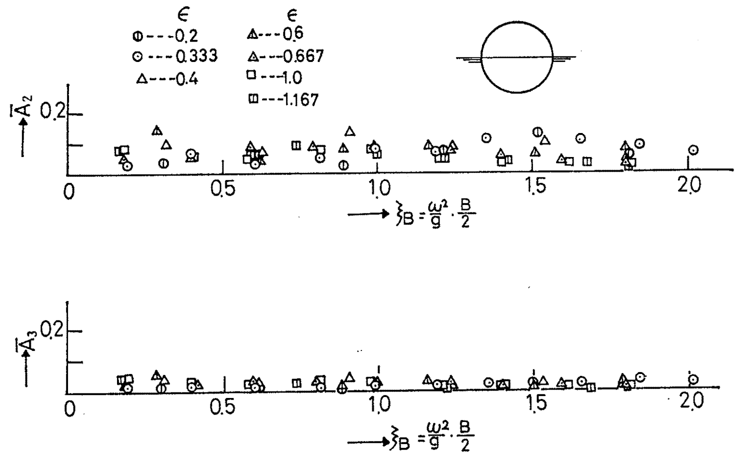

Fig. 53 Ā of second order and third order waves-Circular cylinder

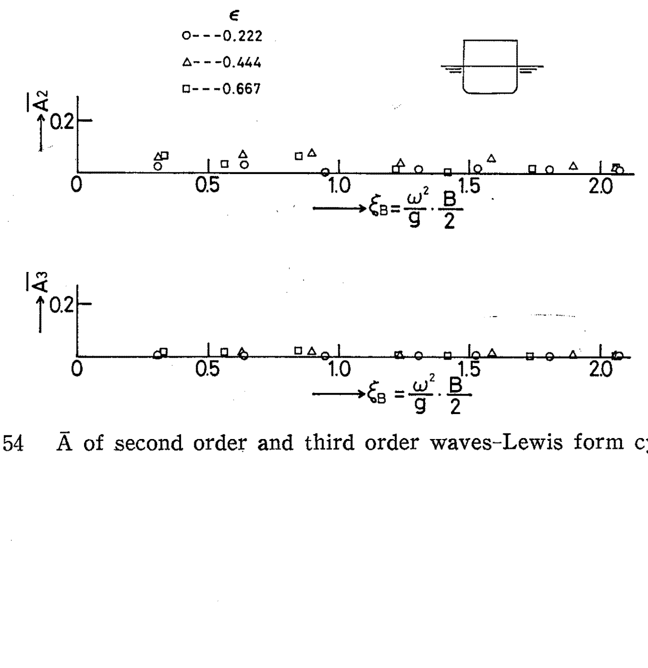

Fig. 54 Ā of second order and third order waves-Lewis form cylinder

Denoting the non-dimensional damping force due to the viscous force by $\bar{N}_{zv}$, we obtain

$$\bar{N}_{zv} = -\frac{|F_{v1}|}{\omega Z_a} \cdot \frac{\sqrt{B/2}}{g\rho B d\sigma L} = \frac{4H_0 \varepsilon C_D \sqrt{\xi_B}}{3\pi\sigma} \tag{16}$$

The wave damping coefficient N_{zw} is given by linear theory as follows

$$\bar{N}_{zw} = \frac{\rho g^2 \bar{A}_1{}^2 \mathrm{L}}{\omega^3} \cdot \frac{\sqrt{B/2}}{g\rho B d\sigma L} = \frac{H_0 \bar{A}_1{}^2}{2\sigma\sqrt{\xi_B{}^3}} \tag{17}$$

Provided that the following relation is assumed to hold

$$\bar{N}_z = \bar{N}_{zv} + \bar{N}_{zw} \tag{18}$$

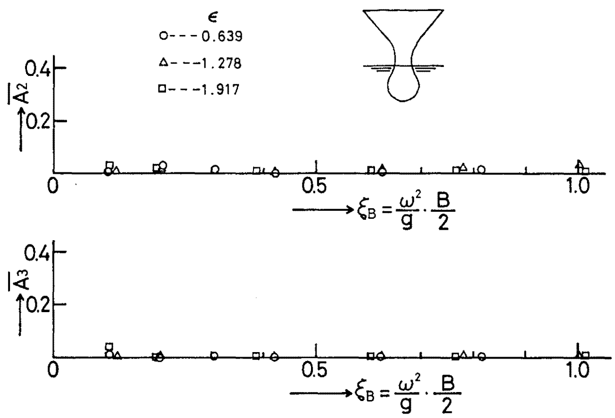

Fig. 55 Ā of second order and third order waves-Bulbous bow cylinder (deep draft)

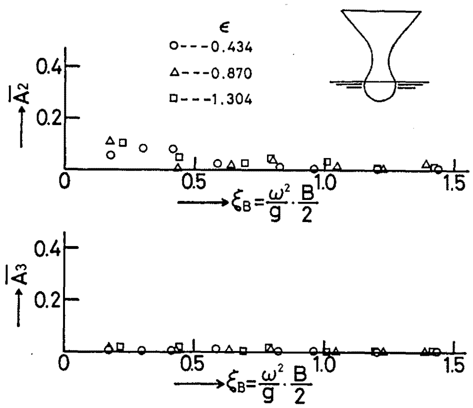

Fig. 56 Ā of second order and third order waves-Bulbous bow cylinder (shallow draft)

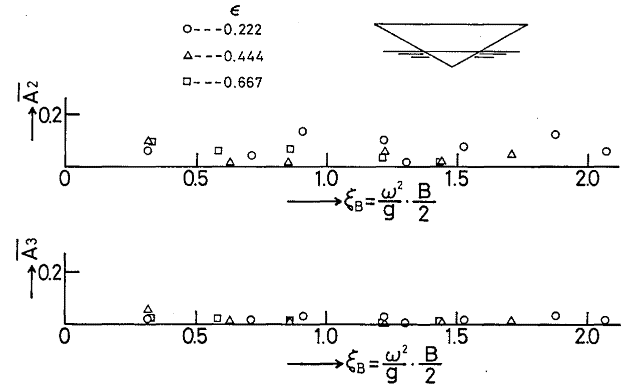

Fig. 57 Ā of second order and third order waves-Triangular cylinder

the drag coefficients C_D are calculated by

$$C_D=\frac{3\pi\sigma}{4H_0\varepsilon\sqrt{\xi_B}}(\bar{N}_z-\bar{N}_{zw}). \tag{19}$$

The calculated values of C_D are presented in Fig. 58~62. The drag coefficients C_D of the circular cylinder in Fig. 58 are rather dispersive in the range of $\xi_B<0.5$ and the dispersion is considered to be caused by the lack of accuracy in experiments. In case of $\xi_B>0.5$, C_D may be considered to be almost constant $(=0.45)$.

The research for the drag force acting on the body in unsteady flow was carried out by Keulegan and Carpenter[13]. They obtained the drag coefficient C_D and the inertia coefficient C_M by measuring the hydrodynamic force acting on the submerged circular cylinder in the standing waves, and they concluded that the important parameter for determining C_D and C_M is τ (Keulegan-Carpenter number) defined by $U_{max}\cdot T/D$, where U_{max} is the

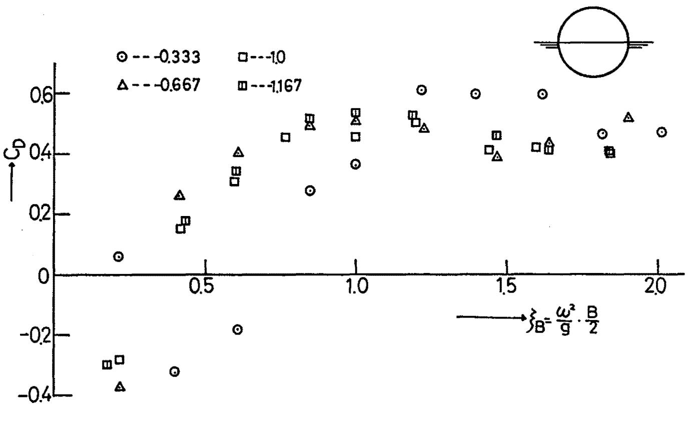

Fig. 58 C_D, Drag coefficient-Circular cylinder maximum velocity of water particles, T the period of standing waves and D the diameter of the circular cylinder. In our report the models were set on the free surface. While, those of Keulegan-Carpenter were in submerged conditions. Nevertheless, we tentatively compare the values of C_D obtained from the present experiments on the circular cylinder with those of Keulegan and Carpenter.

The relations of $U_{max}=\omega Z_a$, $T=\dfrac{2\pi}{\omega}$ lead to $\tau=\pi\varepsilon$, and therefore $0.3<\varepsilon<1.167$ coresponds to $1.0<\tau<3.6$. In the present experiments on the circular cylinder, C_D is neary equal to 0.45. According to them[13], it is equal to

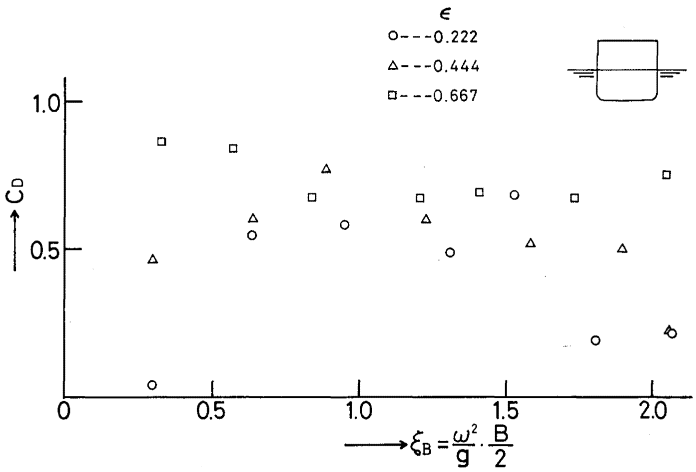

Fig. 59 C_D, Drag coefficient-Lewis form cylinder

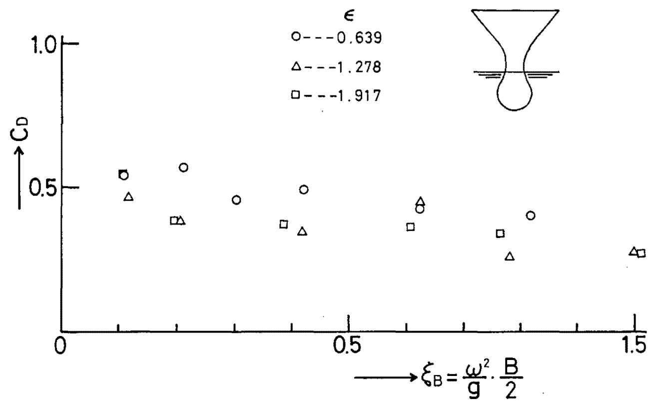

Fig. 60 C_D, Drag coefficient-Bulbous bow cylinder (deep draft)

0.7~1.0 at τ=2.5~3.5. It is supposed that the difference is caused by the model condition, floating and submerged.

The experiments on Lewis form cylinder show that C_D neary equals to 0.6 and is almost constant. As seen from Fig. 60 and 61, C_D of the bulbous bow cylinders depend slightly on ε, and it decreases with the increase of ξ_B. For the bulbous bow cylinders, the variation of C_D of the shallow draft are more remarkable than that of the deep draft. A velocity of the fluid particles is affected by the progressive and the standing waves. It changes with the amplitude and the frequency of the waves. So the depen-

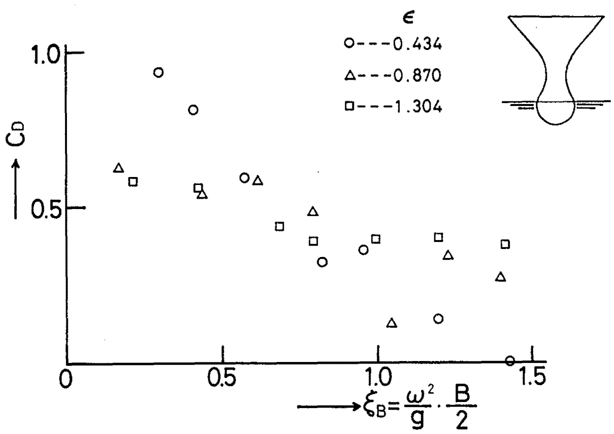

Fig. 61 C_D, Drag coefficient-Bulbous bow cylinder (shallow draft)

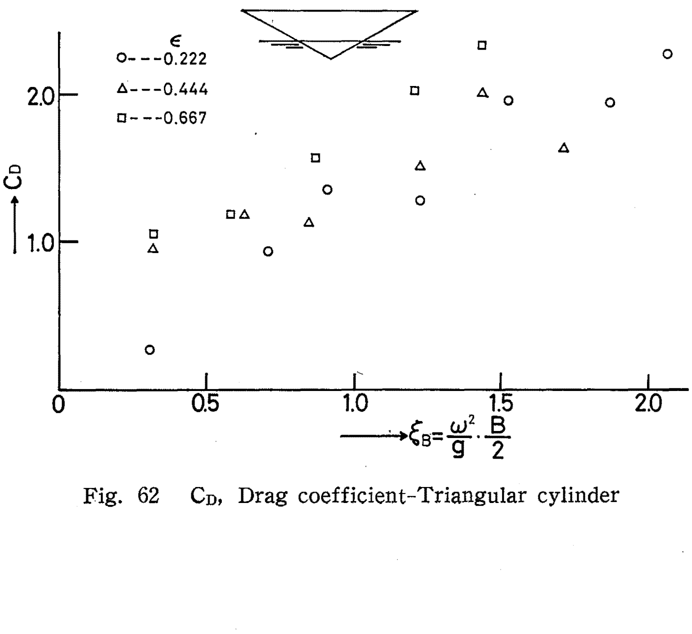

Fig. 62 C_D, Drag coefficient-Triangular cylinder dence of C_D on ε and ξ_B are supposed to be caused by the change of the relative velocity of fluid particles to the model.

On the contrary to the case of the above mentioned cylinders, C_D of the triangular cylinder in Fig. 62 increases with the increase of ξ_B, and it also tends to increase with ε. As for the triangular cylinder, the phenomena of wave breaking and the impact of the model on the water surface are observed through the experiments. The larger ε and ξ_B are, the more remarkable the phenomena are. Therefore, the contents of C_D in the case of the triangular cylinder are differ from those of the other cylinders.

5. Conclusions

Main conclusions obtained from the present investigation are listed below.

1. If added mass coefficients $\bar{M}_z$ are obtained from the measured forces taking account of the non-linearity of the restoring force, experimental values of $\bar{M}_z$ of Lewis form and the bulbous bow cylinders show good agreement with calculated values by linear theory in the wide range of ξ_B and ε. As regards the circular cylinder, the experimental values also show good agreement with the calculated ones in case of $\varepsilon \leqq 0.667$, but the experimental values are larger than the calculated ones where $\varepsilon \geqq 1.0$.

As regards the triangular cylinder, the experimental values of $\bar{M}_z$ show the same tendency as the calculated ones in case of $\varepsilon = 0.222$. However, the experimental values are larger than the calculated ones where $\varepsilon \geqq 0.444$.

2. Experimental values of non-dimensional damping coefficients $\bar{N}_z$ of the cylinders show good agreement with calculated ones by linear theory when ε and ξ_B are as small as the viscous force may be ignored. When ε and ξ_B are not so small, the experimental values of $\bar{N}_z$ of Lewis form and bulbous bow cylinders are larger than the calculated ones on the basis of linear theory, while, for the circular cylinder, the experimental values are smaller than the calculated ones when ε is large and ξ_B is small.

As for the triangular cylinder, the experimental values in case of $\varepsilon < 0.444$ are smaller than the calculated ones, but the experimental values in case of $\varepsilon = 0.667$ abruptly grow larger at $\xi_B = 1.2$.

3. The ratios of the second order force to the first order force, $|F_{w2}|/|F_{w1}|$ are large in case of the triangular, the bulbous bow in shallow draft and the circular cylinder of which water plane areas change appreciably according to the heaving motion. But $|F_{w2}|/|F_{w1}|$ of Lewis form and the bulbous bow cylinder in deep draft are small because their sections are almost wallsided.

4. The ratios of the third order force to the first order force, $|F_{w3}|/|F_{w1}|$ have the same tendency as $|F_{w2}|/|F_{w1}|$.

5. From the comparison between the second order forces obtained from experiments and the calculated ones by perturbation method on the circular cylinder, we obtain two conclusions.

i) In case of small ε, calculated results of time-independent force, periodic force and its phase show fairly good agreement with the experimental ones.

ii) In case of large ε, the calculated values for the second order forces are larger than the experimental ones.

6. In case of not so small ε, damping coefficents calculated by using measured value of $\bar{A}_1$ are much smaller than those obtained from measured forces, and the fact can be reasonably explained by considering not only the wave making force but also the viscous drag force which is propotional to the heaving velocity squared.

As for the triangular cylinder, it is necessary that the impact pressure which arises from the clash of the model against the water surface is considerd in addition to viscous force.

Acknowledgements

We are much indebted to Dr. K. KAWATATE and Dr. M. OHKUSU for valuable discussions and to Mr. M. TAKAKI for help with calculations by linear theory. We would like to thank Mr. T. NAGAHAMA, Mr. T. KITA, Mr. T. SHINOZAKI, Mr. A. TASIRO and Miss. N. SUGINO for contribution to experiments and for assistance in preparing the manuscript.

References

1) Kim, C.H. : "Über den Einflutz nichtlinearer Effekte auf hydrodynamische Kräfte bei erzwungenen Tauchbewegungen prismatischer Körper" Schiffstechnik Heft 73, Sept. 1967.
2) Lee, C.M. : "The Second-Order Theory of Heaving Cylinders in a Free Surface", Journal of Ship Research, Vol. 12, No. 4, Dec. 1968.
3) Parissis, G. : "Second-Order Potentials and Forces for Oscillating Cylinders on a Free Surface", Dissertation, MIT, Report, 66-10, 1966.
4) Potash, R.L. : "Second-Order Thoery of Oscillating Cylinders" Journal of Ship Research, Vol. 15, No. 4, Dec. 1971.
5) Tasai, F. : "Measurements of the Wave Height Produced by the Forced Heaving of the Cylinder", Rep. Res. Inst. Appl. Mech., Vol. VIII, No. 29.
6) Porter, W.R. : "Pressure Distributions, Added-Mass and Damping Coefficients for Cylinders Oscillating in a Free Surface", University of California, Contract Number N-onr-220 (30), July 1960.
7) Paulling, J.R. and Richardson, R.K. : "Measurement of Pressures, Forces, and Radiation Waves for Cylinders in a Free Surface", University of California, Contract Number N-onr-222 (30), June 1962.
8) Vugts, J.H. : "The Hydrodynamic Coefficients for Swaying, Heaving and Rolling Cylinders in a Free Surface", T.N.O. Report, No. 194, 1968.
9) Tasai, F. and Koterayama, W. : "On the nonlinear hydrodynamic forces for heaving circular cylinder on a free surface", J. of SEIBU ZOSENKAI No. 46, 1973, (in Japanese)
10) Koterayama, W. : "Nonlinear hydrodynamic forces acting on cylinders heaving on the surface of a fluid", Bulletin Res. Inst. Appl. Mech., Kyushu Univ., No. 45, 1976, (in Japanese)

11) Ursell, F. :"On the Heaving Motion of a Circular Cylinder on the Surface of a Fluid", Q. T. M. and A. M., Vol. II, 1949.
12) Takaki, M.: "On the Ship Motions in Shallow Water (Part 1)", J, of SEIBU ZOSENKAI, No. 50, 1975, (in Japanese)
13) Keulegan Q. H. and Carpenter, L. H.: "Forces on cylinders and plates in a Oscillating fluid", Journal Res. National Bur. Standards, Vol. 60, No. 5, May 1958.

(Received June 30, 1976)